Chapter 1

The Deuteron and Nuclear Force

"For nuclear physicists, the deuteron should be what the hydrogen atom is for atomic physicists."

K. S. Krane

1.1 Why the deuteron is special

A deuteron is a bound proton–neutron system: the nucleus of deuterium (^{2}H). It is the simplest bound state of nucleons, and therefore an ideal laboratory for the nucleon–nucleon (NN) interaction.

In atomic physics, the hydrogen spectrum taught the Coulomb force and quantum electrodynamics. In nuclear physics one would like a similar study for the deuteron: measure transitions between excited states and read off the force. **Unfortunately there are no bound excited states of the deuteron.** The system is so weakly bound that any excitation puts the proton and neutron into the continuum. All information must therefore come from the ground-state binding energy and size, from ground-state multipoles (spin, magnetic moment, quadrupole moment), and from scattering of free nucleons [6, 2].

Key idea

The deuteron is the hydrogen atom of nuclear physics, with one crucial difference: it has only a ground state. Every number measured is a property of that single state, so the force must be extracted carefully and honestly.

1.2 Binding energy: three independent measurements

The binding energy B_d is known to high precision. Three independent methods agree [6].

1.2.1 Definition

Working always with *atomic* masses (as in Lectures 4–5),

$$B_d = [m(^1\mathrm{H}) + m(n) - m(^2\mathrm{H})]c^2. \tag{1.1}$$

With $c^2 = 931.50\,\text{MeV/u}$, mass differences in atomic mass units convert directly to MeV.

1.2.2 Method 1: mass spectrometry

Mass doublets involving carbon and deuterium compounds fix $m(^2\text{H})$ to better than $10^{-8}\,\text{u}$. Combined with the hydrogen and neutron masses, one finds

$$B_d = 2.22463 \pm 0.00004\,\text{MeV}. \tag{1.2}$$

1.2.3 Method 2: radiative capture

When a free proton and neutron form a deuteron,

$$p + n \to {}^2\text{H} + \gamma, \tag{1.3}$$

the photon energy (minus a small recoil correction) equals B_d. The measured value is $2.224589 \pm 0.000002\,\text{MeV}$, in excellent agreement with the mass-spectroscopic result.

1.2.4 Method 3: photodisintegration

The reverse process,

$$\gamma + {}^2\text{H} \to p + n, \tag{1.4}$$

has a threshold equal to B_d (again corrected for recoil). Experiment gives $2.224 \pm 0.002\,\text{MeV}$.

How weak is "weakly bound"?

Typical mid-mass nuclei have $B/A \sim 8\,\text{MeV}$ (Lecture 4). The deuteron has $B/A \approx 1.11\,\text{MeV}$. It sits far down on the rising part of the B/A curve: almost unbound. That single fact will control everything we calculate below.

For course work we adopt the rounded value used in the original lecture,

$$B_d \approx 2.225\,\text{MeV}, \tag{1.5}$$

which is consistent with all three determinations at the level needed for the square-well analysis.

1.3 A simple model: the square well

1.3.1 Why a square well?

The true NN potential is complicated: a repulsive core at short distance, a strong attraction at $\sim 1\,\text{fm}$, a pion-exchange tail at larger r, and spin- and tensor-dependent pieces (Lectures 7–9). To learn the *scale* of the force we represent the interaction by a three-dimensional square well in the relative coordinate $r = |\boldsymbol{r}_p - \boldsymbol{r}_n|$:

$$V(r) = \begin{cases} -V_0, & r < R, \\ 0, & r > R. \end{cases} \tag{1.6}$$

Here r is the proton–neutron separation and R is the *radial range*: the attraction acts for separations $r < R$. It is neither a nucleon radius nor the deuteron rms charge radius, and it is not a diameter. We adopt the explicit toy-model convention $R = 2.00\,\text{fm}$; the measured B_d then fixes V_0.

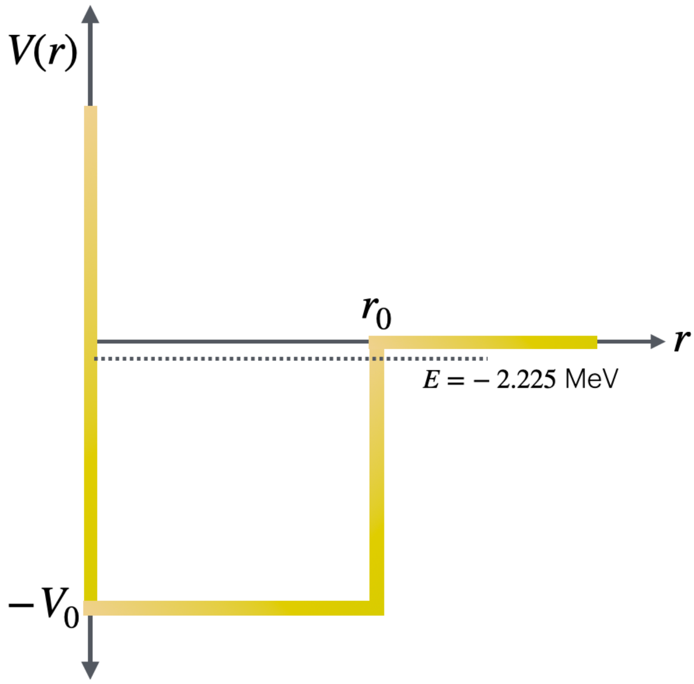

Figure 1.1: Square-well model of the NN potential (lecture figure). Inside $r < R$ the potential is $-V_0$; outside it vanishes. The deuteron energy $E = -B_d$ lies just below threshold.

1.3.2 Reduced mass and the radial equation

The two-body problem with equal masses $m_p \approx m_n \approx m_N$ reduces to a one-body problem with reduced mass

$$\mu = \frac{m_p m_n}{m_p + m_n} \approx \frac{m_N}{2}. \tag{1.7}$$

For a central potential we write the wave function as $\psi(\boldsymbol{r}) = Y_{\ell m}(\hat{r})\, u(r)/r$. The radial function $u(r)$ obeys

$$-\frac{\hbar^2}{2\mu}\frac{\mathrm{d}^2 u}{\mathrm{d}r^2} + \left[V(r) + \frac{\ell(\ell+1)\hbar^2}{2\mu r^2}\right] u = Eu. \tag{1.8}$$

Assumption (to be checked later): the ground state has $\ell = 0$, by analogy with the hydrogen $1s$ state. Then the centrifugal term vanishes and (1.8) looks exactly like a one-dimensional Schrödinger equation on the half-line $r > 0$.

1.3.3 Interior and exterior solutions

With $E = -B_d < 0$, define

$$k = \frac{1}{\hbar}\sqrt{2\mu(V_0 - B_d)} \qquad (r < R), \tag{1.9}$$

$$\gamma = \frac{1}{\hbar}\sqrt{2\mu B_d} \qquad (r > R). \tag{1.10}$$

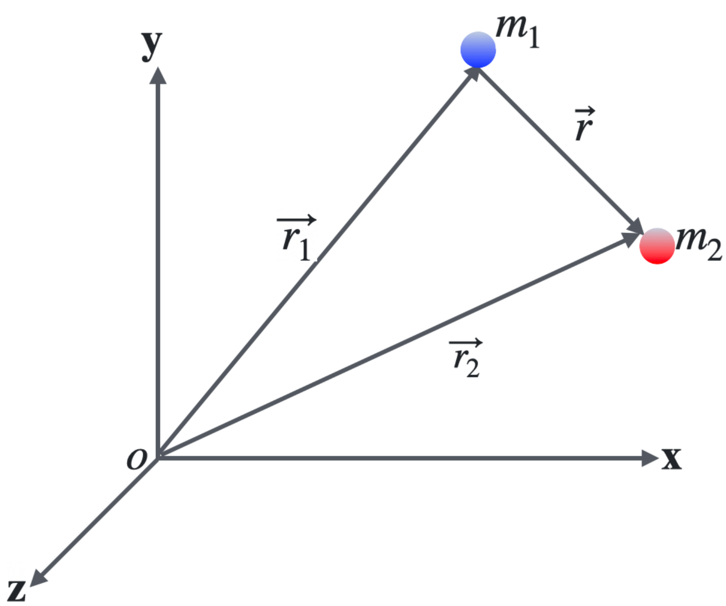

Figure 1.2: Relative coordinate of proton and neutron. The square well acts on this separation; the centre of mass moves freely.

Equivalently,

$$k = \frac{\sqrt{2\mu(V_0 + E)}}{\hbar}, \qquad E = -B_d.$$

For $\mu \approx m_N/2$, the useful numerical coefficient is $\hbar^2/(2\mu) \approx 41.5\,\mathrm{MeV\,fm}^2$.

Inside the well the general solution is

$$u(r) = A\sin(kr) + B\cos(kr). \tag{1.11}$$

Boundary condition at the origin: ψ must remain finite, so $u(0) = 0$. That forces $B = 0$:

$$u(r) = A\sin(kr), \qquad r < R. \tag{1.12}$$

Outside the well,

$$u(r) = Ce^{-\gamma r} + De^{+\gamma r}. \tag{1.13}$$

Boundary condition at infinity: u must not explode, so $D = 0$:

$$u(r) = Ce^{-\gamma r}, \qquad r > R. \tag{1.14}$$

1.3.4 Matching: the transcendental condition

The physical content of the bound-state problem is fixed by the finite range of the force and by quantum mechanics. Outside the well there is no attraction, so a bound system ($E = -B_d < 0$) can exist only because the wave function tunnels under the continuum; the exterior solution must decay exponentially. Inside the well the nucleons feel a constant attraction $-V_0$, so the radial function oscillates. Matching the two regions at $r = R$ quantises the allowed (V_0, R) pairs that reproduce the measured binding energy [6, 13].

Write

$$V(r) = \begin{cases} -V_0 & r < R, \\ 0 & r > R, \end{cases} \qquad E = -B_d < 0.$$

For $r < R$ the radial Schrödinger equation becomes

$$-\frac{\hbar^2}{2\mu}\frac{\mathrm{d}^2 u}{\mathrm{d}r^2} - V_0 u = Eu \quad \Rightarrow \quad \frac{\mathrm{d}^2 u}{\mathrm{d}r^2} = -k^2 u,$$

with wave number

$$k = \frac{\sqrt{2\mu(V_0 - B_d)}}{\hbar} = \frac{\sqrt{2\mu(V_0 + E)}}{\hbar}, \tag{1.15}$$

where the second form uses $E = -B_d$ so that $V_0 - B_d = V_0 + E$ (not $V_0 + |E|$ written as a separate definition: since $E = -B_d$, one has $V_0 + E = V_0 - B_d$). Both expressions are identical; they are not two different physical definitions. The general interior solution is $u_{\mathrm{I}}(r) = A\sin(kr) + B\cos(kr)$. Because $\psi = u/r$ must remain finite at the origin, $u(0) = 0$, which forces $B = 0$:

$$u_{\mathrm{I}}(r) = A\sin(kr). \tag{1.16}$$

Physically this is the statement that there is no source of probability current at $r = 0$; the relative wave function vanishes at vanishing separation in the s-wave radial problem.

Outside the well, $V = 0$ and $E = -B_d$, so

$$\frac{\mathrm{d}^2 u}{\mathrm{d}r^2} = \gamma^2 u, \qquad \gamma = \frac{\sqrt{2\mu B_d}}{\hbar}.$$

The exterior solution is $u_{\mathrm{II}}(r) = Ce^{-\gamma r} + De^{+\gamma r}$. The growing exponential is discarded so that the state is normalisable:

$$u_{\mathrm{II}}(r) = Ce^{-\gamma r}. \tag{1.17}$$

The decay length $1/\gamma$ is large when B_d is small: weak binding means the nucleons spend much of their time *outside* the range of the force, which is why the deuteron rms radius exceeds the naive well radius.

Continuity of ψ and of $\mathrm{d}\psi/\mathrm{d}r$ at the edge of a finite square well requires continuity of u and u' at $r = R$:

$$A\sin(kR) = Ce^{-\gamma R}, \tag{1.18}$$

$$Ak\cos(kR) = -C\gamma e^{-\gamma R}. \tag{1.19}$$

Dividing these two equations eliminates the unknown amplitudes A and C and yields the matching condition

$$k\cot(kR) = -\gamma. \tag{1.20}$$

Equation (1.20) is transcendental: once R and B_d are fixed, it determines the depth V_0 that can support the observed bound state. That is the quantitative link between the measured binding energy and the strength of the residual force.

1.3.5 Amplitude matching and normalisation

The first matching equation gives

$$C = A\sin(kR)e^{\gamma R}. \tag{1.21}$$

For the convention $\int_0^\infty |u(r)|^2\,\mathrm{d}r = 1$, the common interior amplitude is therefore fixed by writing $C = A\sin(kR)e^{\gamma R}$ and evaluating each piece:

$$\int_0^R \sin^2(kr)\,\mathrm{d}r = \int_0^R \frac{1-\cos(2kr)}{2}\,\mathrm{d}r = \frac{R}{2} - \frac{\sin(2kR)}{4k}, \tag{1.22}$$

$$\int_R^\infty e^{-2\gamma r}\,\mathrm{d}r = \frac{e^{-2\gamma R}}{2\gamma}, \tag{1.23}$$

so that

$$\begin{aligned} 1 &= A^2 \int_0^R \sin^2(kr)\,\mathrm{d}r + C^2 \int_R^\infty e^{-2\gamma r}\,\mathrm{d}r \\ &= A^2 \left[\frac{R}{2} - \frac{\sin(2kR)}{4k}\right] + A^2 \sin^2(kR)\,e^{2\gamma R} \cdot \frac{e^{-2\gamma R}}{2\gamma} \\ &= A^2 \left[\frac{R}{2} - \frac{\sin(2kR)}{4k} + \frac{\sin^2(kR)}{2\gamma}\right]. \end{aligned} \tag{1.24}$$

Thus A is the inverse square root of the bracket and C follows from continuity. The probability beyond the force range is

$$P_> = \frac{A^2 \sin^2(kR)}{2\gamma}. \tag{1.25}$$

As $B_d \to 0^+$, $\gamma \to 0^+$, the exterior term dominates the norm: the state becomes spatially large even though the force range stays fixed. At threshold $\gamma = 0$, matching requires $kR = \pi/2$ for the first state, or $V_0 R^2 = \pi^2\hbar^2/(8\mu)$.

1.4 Numerical result for the adopted toy range

Electron scattering gives an rms charge radius of the deuteron of about 2.1 fm. That is *not* the force range: it is a charge-weighted rms distance from the centre of mass. The pn separation, matter radius, charge radius, and square-well range are distinct definitions. For the adopted teaching model $R = 2.00\,\mathrm{fm}$, with $B_d = 2.2246\,\mathrm{MeV}$ and $\hbar^2/(2\mu) \approx 41.5\,\mathrm{MeV\,fm^2}$, one solves (1.20) as follows.

Define the dimensionless quantities

$$\xi \equiv kR, \qquad \eta \equiv \gamma R = R\sqrt{\frac{2\mu B_d}{\hbar^2}}. \tag{1.26}$$

For $R = 2.00\,\mathrm{fm}$,

$$\eta = 2.00\sqrt{\frac{2.2246}{41.5}} \approx 2.00 \times 0.232 \approx 0.463.$$

The matching condition $k\cot(kR) = -\gamma$ becomes $\xi \cot \xi = -\eta$, or

$$\xi \cot \xi = -0.463. \tag{1.27}$$

The relevant root in $(\pi/2, \pi)$ is $\xi = 1.820$. Then

$$V_0 - B_d = \frac{\hbar^2 k^2}{2\mu} = \frac{\hbar^2}{2\mu}\frac{\xi^2}{R^2} = 41.5 \cdot \frac{(1.820)^2}{(2.00)^2} \approx 34.4\,\mathrm{MeV}, \tag{1.28}$$

$$V_0 = 34.4 + 2.2246 \approx 36.6\,\mathrm{MeV}. \tag{1.29}$$

$$V_0 \approx 36.6\,\mathrm{MeV} \qquad (R = 2.00\,\mathrm{fm}). \tag{1.30}$$

Equation (1.20) constrains a curve in the (R, V_0) plane, not a unique pair: one observable (B_d) cannot fix two potential parameters. Our quoted depth is conditional on the labelled $R = 2.00$ fm convention; a shorter range requires a deeper well. The residual NN attraction sampled by the deuteron is tens of MeV deep on a fermi scale, barely enough to bind [6, 13].

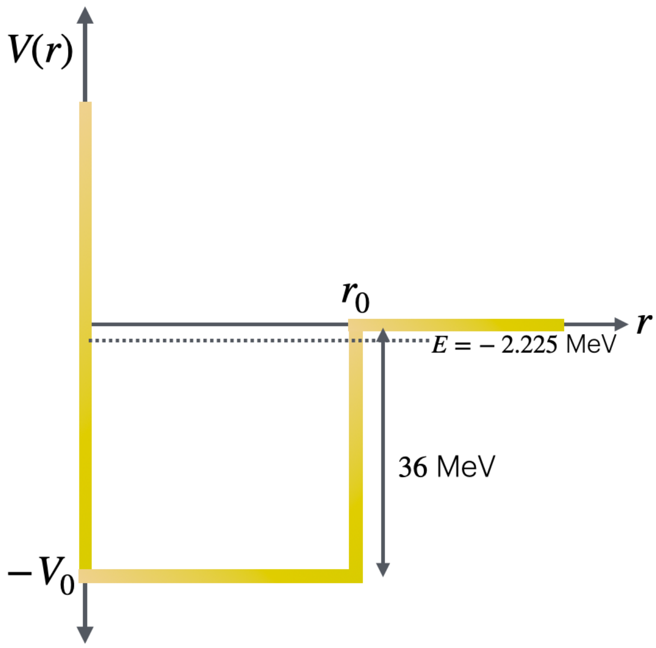

Figure 1.3: Lecture figure emphasising the depth V_0 needed to bind the deuteron. The bound level sits only ~ 2.2 MeV below the continuum, so most of the well depth is cancelled by kinetic energy of confinement.

Key idea

Barely bound. The energy $E = -B_d$ lies just below the top of the well. If the force were slightly weaker, or the range slightly smaller, there would be no bound state at all. The wave function barely "turns over" inside the well so that it can match a decaying exponential outside [6].

Why this matters for the Sun and the early universe

Deuterium formation is the first step in the solar *pp* chain and in Big Bang nucleosynthesis. If no stable two-nucleon bound state existed, heavier nuclei would not form in the early universe and stellar hydrogen burning would not begin as it does. The weak binding of the deuteron is a threshold fact about the world we inhabit [6].

Remark

Because the binding is weak, the probability of finding the nucleons *outside* the range R is large. The exponential tail extends far; low-energy NN scattering is correspondingly sensitive to the asymptotic normalisation. A large fraction of the time is spent outside the well [2].

1.5 Residual force: why nucleons attract at all

Before leaving the central model, place the force in a modern context. Nucleons are not elementary: $p = uud$, $n = udd$. The fundamental strong interaction (QCD) confines colour. Colour-neutral nucleons still interact at short distance through a residual force, much as neutral atoms form molecules through residual electromagnetic multipoles.

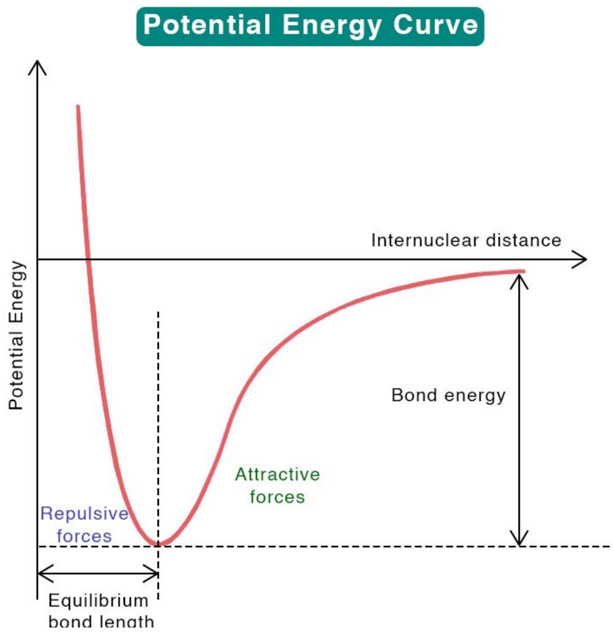

Figure 1.4: Molecular analogy: short-range repulsion, attractive well, finite range. Colour-neutral nucleons interact through residual colour forces on the fermi scale in a similar qualitative way.

Yukawa's meson exchange (1935) explains the long-range tail: the force range is of order $\hbar/(m_\pi c) \sim 1.4\,\text{fm}$. The square well is a teaching caricature of that attraction plus short-range repulsion. Lectures 7–9 will show that even this picture is incomplete: the force depends on spin and contains a non-central (tensor) piece.

1.6 What we have learned, and what we have not

1. The deuteron binding energy is $B_d \approx 2.224\,\text{MeV}$, measured three independent ways.
2. There are no bound excited states: the system is barely bound.
3. The labelled teaching choice $R = 2.00\,\text{fm}$ requires depth $V_0 \approx 36.6\,\text{MeV}$; shorter range needs deeper V_0.
4. That depth sets the scale of the NN attraction underlying the SEMF volume term a_V (Lecture 4).
5. We have *assumed* $\ell = 0$. Spin, magnetic moment, and quadrupole moment will test that assumption (Lectures 8–9).

Takeaway

In this lecture and the next.

- This lecture: binding energy and a central well $\Rightarrow$ force range and depth.
- Next lecture: I^π and $\mu_d \Rightarrow$ spin dependence and a few-percent D-wave.
- Lecture after: $Q_d \neq 0 \Rightarrow$ tensor (non-central) force.

Only after those three steps is the qualitative NN force complete for PH5001.

1.7 Deeper physics: weak binding and the asymptotic wave function

1.7.1 No bound excited states

Unlike the hydrogen atom, the deuteron has **no bound excited states**. Any excitation exceeds B_d and produces a free $p + n$ pair in the continuum. All structure information must therefore come from the ground-state multipoles (Lectures 8–9) and from scattering (phase shifts), not from a discrete spectrum [6, 2].

1.7.2 Wave function mostly outside the well

With the lecture convention $V_0 = 36.6\,\text{MeV}$ and $R = 2.00\,\text{fm}$, the matching condition $k\cot(kR) = -\gamma$ places the eigenenergy just below threshold. The exterior decay constant $\gamma = \sqrt{2\mu B_d}/\hbar$ is small ($\gamma^{-1} \approx 4.3\,\text{fm}$), so the exponential tail extends far: the two nucleons spend a large fraction of the time *outside* the range of the force. That is why the rms charge radius ($\sim 2.1\,\text{fm}$ from electron scattering) is not a direct measure of the force range, and why low-energy NN scattering is so sensitive to the asymptotic normalisation.

Range vs depth degeneracy

Fixing only B_d leaves a curve of allowed (R, V_0). Scattering lengths and effective ranges (Lecture 10) break that degeneracy by adding low-energy continuum information. A single bound-state energy never determines a unique potential.

Remark

Exterior dominance and capture. Because $P_> \sim 0.5$–0.7, radiative np capture at thermal energies and low-energy np scattering are controlled by the same long tail that sets $r_{\rm rms}$. A deep interior well can be replaced by a different V_0 without changing low-energy observables if the asymptotic γ and normalisation are held fixed. That is why modern analyses quote scattering lengths and asymptotic normalisation constants alongside B_d [6, 14].

1.7.3 Square well as a teaching potential

Realistic potentials (Yukawa one-pion tail, hard or soft core at short distance, tensor and spin–orbit terms) are more complex. The square well is retained because:

- it is analytically solvable for $L = 0$;
- it returns $V_0 = 36.6\,\mathrm{MeV}$ for the labelled $R = 2.00\,\mathrm{fm}$ choice, the correct scale;
- it makes the near-threshold character of the bound state obvious.

Lectures 8–9 show why a pure central well is still incomplete: spin and quadrupole data demand a tensor component.

1.8 Square-well matching: from algebra to exterior probability

1.8.1 Interior and exterior solutions

The lecture derives the bound-state condition by matching $u(r) = r\psi(r)$ and its derivative at $r = R$. Inside the well ($E < 0$, $V = -V_0$) the solution is oscillatory,

$$u_{\rm in}(r) = A\sin(kr), \qquad k = \frac{\sqrt{2\mu(V_0 - B_d)}}{\hbar}, \tag{1.31}$$

while outside it decays exponentially with

$$u_{\rm out}(r) = Be^{-\gamma r}, \qquad \gamma = \frac{\sqrt{2\mu B_d}}{\hbar}. \tag{1.32}$$

Continuity of u and u' at $r = R$ eliminates A/B and yields $k\cot(kR) = -\gamma$. Physically, the interior wave must “turn over” just enough that the logarithmic derivative matches the decay slope imposed by B_d. Because $B_d \ll V_0$, one has $kR \approx \pi/2$ (just below the first quarter-wave threshold) and $\gamma R \ll 1$: the bound state sits in the corner of parameter space where the well is deep but the eigenenergy is shallow.

1.8.2 A worked estimate of the exterior fraction

Take $B_d = 2.22\,\mathrm{MeV}$, $\mu = m_N/2$, and $\hbar c = 197\,\mathrm{MeV\,fm}$. Then

$$\gamma^{-1} = \frac{\hbar}{\sqrt{2\mu B_d}} \approx \frac{197}{\sqrt{938 \times 2.22}} \approx 4.3\,\mathrm{fm}, \tag{1.33}$$

comparable to the deuteron rms radius. With $R = 2.00\,\mathrm{fm}$ and a typical normalisation, the probability outside the well is

$$P_{>} \approx \frac{\displaystyle\int_R^\infty u^2\,\mathrm{d}r}{\displaystyle\int_0^\infty u^2\,\mathrm{d}r} \sim 0.5\text{–}0.7, \tag{1.34}$$

depending on the precise V_0 fit. Most of the wave function therefore samples the force *beyond* its nominal range: low-energy NN physics is controlled by the asymptotic tail, not by the interior where V_0 is large. That is the same halo logic seen later for light nuclei (Lecture 1 further material), but here it appears in the simplest two-body bound state.

Threshold arithmetic

The quantum condition for one s-wave bound state, $V_0R^2 > \pi^2\hbar^2/(8\mu) \approx 109\,\mathrm{MeV\,fm}^2$, separates bound from unbound channels. The triplet deuteron clears it ($\sim 140\,\mathrm{MeV\,fm}^2$); the singlet ${}^1S_0$ channel falls just short ($\sim 93\,\mathrm{MeV\,fm}^2$). Spin dependence is therefore not a matter of sign reversal but of depth crossing a quantitative threshold [6, 14].

Remark

Limits of the square well. The model ignores the tensor force (Lecture 9), spin–orbit terms, and the long-range one-pion tail (Lecture 11). It also hides the fact that realistic potentials have a repulsive core at $r \lesssim 0.5\,\mathrm{fm}$. Its value is pedagogical transparency: one sees directly how weak binding inflates r_{rms} and why scattering data (Lecture 10) are mandatory to fix the potential beyond a single binding energy.

1.8.3 Reading the matching condition graphically

Define $f(kR) = kR\cot(kR) + \gamma R$. A bound state exists when $f(kR) = 0$. As $B_d \to 0$, $\gamma \to 0$ and the solution approaches $kR = \pi/2$ from below. Increasing B_d increases γR and pulls kR slightly below $\pi/2$, deepening the interior oscillation. Plotting $V_0(R)$ for fixed B_d produces a family of acceptable wells: shallow and wide, or deep and narrow. Only additional data (phase shifts in Lecture 10, tensor observables in Lectures 8–9) select a member of that family. The square well therefore teaches *qualitative* weak-binding physics and *quantitative* threshold arithmetic, but not a unique microscopic potential [2, 6].

Key idea

Weak-binding checklist (Lecture 7).

- Matching: $k\cot(kR) = -\gamma$ with $\gamma = \sqrt{2\mu B_d}/\hbar$.

- Exterior: $P_> \sim 0.5$–0.7, $r_{\rm rms} > R$.
- Threshold: $V_0 R^2 \gtrsim 109\,\mathrm{MeV\,fm^2}$ for one s-wave bound state.
- Beyond B_d: need μ_d, Q_d, and a_t (Lectures 8–10).

1.9 Further physics: only one bound NN state

There is only one bound $A = 2$ nucleus, the deuteron, and it has no bound excited states. Its binding energy is only $B_d \approx 2.225\,\mathrm{MeV}$, so any excitation puts the system into the $p + n$ continuum [14, 6, 13]. That single fact forces the entire multipole programme of Lectures 7–9: structure information must come from ground-state moments and from scattering, not from a discrete spectrum.

Modern NN potentials also include three-nucleon forces, which have no classical two-body analogue and are hard to fix from scattering alone [13, 4]. For PH5001 the two-body square well and the tensor force extracted from the deuteron remain the essential lessons.

At the QCD level, the residual nucleon–nucleon force is the long-distance face of a theory in which the strong coupling *grows* toward large distance (confinement) and becomes weak at short distance (asymptotic freedom) [15, 4]. Yukawa's pion sets the range $\sim$ 1–2 fm of the residual force used in this chapter.

1.9.1 Bound-state condition for a square well

For an s-wave square well of depth V_0 and range R,

$$V(r) = \begin{cases} -V_0 & r < R, \\ 0 & r > R, \end{cases} \tag{1.35}$$

the radial function $u(r) = r\psi(r)$ oscillates inside the well and decays as $e^{-\kappa r}$ outside, with

$$k = \frac{\sqrt{2\mu(V_0 + E)}}{\hbar}, \qquad \kappa = \frac{\sqrt{-2\mu E}}{\hbar}, \qquad E = -B_d < 0. \tag{1.36}$$

Matching u and u' at $r = R$ yields

$$k\cot(kR) = -\kappa. \tag{1.37}$$

The first bound state appears when the exterior decay constant vanishes, $\kappa \to 0^+$, so $\cot(kR) \to 0^-$ and

$$kR = \frac{\pi}{2} \qquad \text{(threshold)}. \tag{1.38}$$

At $E = 0$ one has $k = \sqrt{2\mu V_0}/\hbar$, hence at least one bound state requires

$$V_0 R^2 > \frac{\pi^2\hbar^2}{8\mu} \approx 109\,\mathrm{MeV\,fm^2} \tag{1.39}$$

($\mu \approx m_N/2$). Fitting the deuteron gives approximately

$$V_0 R^2 (s{=}1) \approx 140\,\mathrm{MeV\,fm^2}, \tag{1.40}$$

while low-energy *np* scattering in the singlet channel yields

$$V_0 R^2(s{=}0) \sim 90\text{–}95\,\mathrm{MeV\,fm}^2 \tag{1.41}$$

just *below* threshold. Typical phenomenological values are $V_0 \approx 47\,\mathrm{MeV}$, $R \approx 1.7\,\mathrm{fm}$ (triplet) and a shallower, wider singlet well [14, 6].

Because B_d is small, the exterior decay length $1/\kappa$ is long. Normalising the asymptotic wave $u(r) \sim Ae^{-\kappa r}$ for $r > R$, the probability outside the well is

$$P_> = \frac{\displaystyle\int_R^\infty A^2 e^{-2\kappa r}\,\mathrm{d}r}{\displaystyle\int_0^\infty u^2\,\mathrm{d}r} \sim \frac{A^2 e^{-2\kappa R}/(2\kappa)}{\text{total norm}}, \tag{1.42}$$

which is of order 50%–70% for the deuteron: most of the probability density sits *outside* the range of the force, and the rms radius exceeds R.

1.9.2 No *nn* or *pp* bound states and charge independence

Charge independence of the strong force, together with the Pauli principle, explains why only *pn* binds: the $s = 1$, $\ell = 0$ state is allowed for *pn* but forbidden for identical *nn* or *pp*; the $s = 0$ channel is unbound for all three pairs [14]. Mirror binding differences such as ^{3}H vs ^{3}He are then mostly Coulomb.

The naive reading "attractive in $s = 1$, repulsive in $s = 0$" is wrong: both channels are attractive; only the triplet is deep enough to bind [14, 6].

1.9.3 Yukawa potential and pion range

A more realistic long-range form is

$$V(r) = g\,\frac{\hbar c}{r}\,e^{-r/r_0}, \qquad r_0 = \frac{\hbar}{m_\pi c} \approx 1.4\,\mathrm{fm}. \tag{1.43}$$

Yukawa predicted the pion mass from the force range [9, 14, 5]. In Born approximation the Fourier transform of the Yukawa potential is the propagator

$$M(q^2) \propto \frac{1}{q^2 + m_\pi^2 c^2}, \tag{1.44}$$

which reduces to a contact interaction when $m_\pi \to \infty$ (zero range). Short-range repulsion ("hard core") and multi-meson exchanges complete modern NN potentials [14, 15].

The same Yukawa logic, applied to the weak interaction with a heavy mediator, explains why the weak force looks feeble at low energy even though its underlying coupling is not tiny: $G_F \propto g^2/m_W^2$ [5]. For the strong residual force the light pion makes the range nuclear, not subnuclear.

1.9.4 Photodisintegration and the binding energy

The deuteron binding energy is measured to high precision from the threshold for

$$\gamma + {}^{2}\mathrm{H} \to p + n, \tag{1.45}$$

and from the reverse radiative capture. The photon energy must supply at least $B_d \approx 2.224\,\mathrm{MeV}$ (plus a small centre-of-mass correction). That B_d is only $\sim 0.1\%$ of the rest energy of the deuteron: the system is barely bound, which is why the wave function leaks so far outside the well [6, 14].

1.9.5 Why scattering is needed

With only one bound state, the deuteron samples the NN force mainly in the ${}^3S_1$–${}^3D_1$ channel at a fixed average separation. Nucleon–nucleon scattering (especially on hydrogen targets, to avoid multiple scattering inside a heavy nucleus) maps other partial waves, energies, and spin orientations. Phase shifts then constrain the full potential used in few-body and many-body calculations [6, 4].

1.9.6 Triplet vs singlet wells in numbers

Phenomenological square-well fits that also use low-energy scattering give distinct wells in the two spin channels [14]:

Channel	V_0 (MeV)	R (fm)	V_0R^2 (MeV fm^2)
Triplet $s = 1$ (bound)	46.7	1.73	≈ 140
Singlet $s = 0$ (unbound)	12.5	2.79	≈ 93.5
Threshold for one bound state			109

Both channels are attractive; only the triplet clears the quantum threshold $V_0R^2 > 109\,\mathrm{MeV\,fm}^2$. That is the quantitative content of "spin-dependent nuclear force" at the square-well level.

1.9.7 Normalisation and the asymptotic constant

The exterior wave $u(r) \sim Ae^{-\gamma r}$ defines the **asymptotic normalisation constant** A, which sets the absolute scale of the np capture cross section and of the deuteron photo-disintegration amplitude. Low-energy NN scattering fixes the *ratio* of phase shifts (Lecture 10) but not A without a normalisation convention. In practice A is tied to the deuteron rms radius and to $\eta_D = a_D/a_S$, the D/S ratio at large r (Lecture 9). The square well makes the point transparent: a shallow bound state forces a long tail ($\gamma^{-1} \gg R$), so observables sensitive to the wave function at $r \sim 5$–$10\,\mathrm{fm}$ (the electromagnetic radius, capture at thermal energies) depend on the *exterior* shape even though the binding energy is fixed by the interior matching.

Rms radius from weak binding

A crude estimate treats the deuteron as a sphere of radius $r_{\mathrm{rms}} \approx 2.1\,\mathrm{fm}$. Compare with the force range $R \sim 2\,\mathrm{fm}$: the rms radius exceeds the well radius because $P_> \sim 0.5$–0.7. For a deeply bound state ($B \sim 30\,\mathrm{MeV}$), $\gamma^{-1} \lesssim 1\,\mathrm{fm}$ and r_{rms} would track R. The deuteron is the opposite limit, foreshadowing halo nuclei in Lecture 1 further material.

1.9.8 Bridge to Lectures 8–10

Lecture 7 fixes the *existence* and *weakness* of the NN bound state. Lecture 8 asks what magnetic moment that state carries; Lecture 9 asks whether the charge distribution is spherical. Neither question is answered by B_d alone. Lecture 10 adds continuum phase shifts in the singlet and triplet channels, breaking the (R, V_0) degeneracy of the square well. Together, bound and scattering data constrain the same underlying potential, with the deuteron sampling only the triplet, near-threshold corner of the full parameter space [6, 14].

1.9.9 Levinson threshold and the singlet channel

Levinson's theorem links the number of bound states to $\delta_0(0)$. The triplet channel has one bound state (deuteron), so $\delta_0^{(t)}(0) = +\pi/2$ and $a_t > 0$. The singlet channel has none, so $\delta_0^{(s)}(0) = 0$ and $a_s < 0$ with $|a_s| \gg R$: the virtual ${}^1S_0$ state sits just above threshold (Lecture 10). The square-well threshold $V_0 R^2 \gtrsim 109\,\mathrm{MeV\,fm}^2$ quantifies how close the singlet well falls short ($\sim 93\,\mathrm{MeV\,fm}^2$). Spin dependence is therefore a quantitative depth difference, not a sign flip of the force.

1.9.10 Capture cross section and the long tail

Radiative np capture at thermal energies proceeds through an s-wave np collision and emission of a real photon. The cross section scales with the square of the asymptotic wave function at the origin and with $1/v$ (standard $1/v$ law for slow neutrons). Because the deuteron wave function extends to $\sim 5\,\mathrm{fm}$, the capture rate is enhanced relative to a compact bound state of the same B_d. This is another manifestation of exterior dominance: weak binding inflates the tail, which controls both scattering lengths (Lecture 10) and radiative processes [6, 14].

1.10 Deeper reading: matching, asymptotic normalisation, and halos

The square-well deuteron of Lecture 7 is solved by matching logarithmic derivatives at the well radius R. Writing $\gamma = \sqrt{2\mu B_d}/\hbar$ for the exterior decay constant, the asymptotic wave function $u(r) \propto e^{-\gamma r}$ dominates the normalisation when B_d is small. The exterior probability

$$P_> = \int_R^\infty |u|^2\,\mathrm{d}r \Big/ \int_0^\infty |u|^2\,\mathrm{d}r \tag{1.46}$$

approaches unity as $B_d \to 0$: that is the halo limit. For the physical deuteron, $B_d = 2.224\,\mathrm{MeV}$ and $P_>$ is already large, which is why low-energy np scattering and the deuteron radius are tightly linked through the scattering length (Lecture 10).

A one-parameter well that fits only B_d cannot predict both the radius and the D-wave quadrupole moment (Lectures 8–9). Effective field theory reorganises that underdetermination into a power counting with truncation errors. The pedagogical moral remains: weak binding amplifies long-distance physics and suppresses sensitivity to short-distance details, until observables that probe the tensor force or short-range currents are considered.

Connect forward: the same exterior dominance appears in halo nuclei near drip lines (Lecture 13) and in the need for continuum coupling in reactions (Lecture 21). Connect back: saturation in Lecture 2 requires attractions strong enough to bind bulk matter, yet the deuteron remains only weakly bound because of the spin–isospin structure of the force.

Effective range and asymptotic normalisation

The asymptotic normalisation coefficient (ANC) of the deuteron wave function controls peripheral transfer reactions that attach a proton or neutron to a target (Lecture 21). Because the exterior wave is fixed by B_d and the scattering length, ANCs are more stable than short-range spectroscopic factors when the reaction is peripheral. Students should connect the Lecture 7 matching condition to that exterior normalisation before treating transfer as a pure structure measurement.

Tensor force preview

Even before Lecture 9, note that a central square well cannot generate a quadrupole moment. Any observable sensitive to tensor structure (Q_d, some polarisation observables) requires physics beyond the toy well. Keep a list of which deuteron observables are long-distance dominated (B_d, radius, scattering length) and which need interior tensor physics (μ_d details, Q_d, photodisintegration at higher energy).

Three-body force teaser

The triton and ^{3}He binding energies cannot be reproduced from two-body forces alone fitted to NN scattering. That fact, matured in Lecture 11, already warns that the deuteron's success as a two-body system does not license a pure two-body description of bulk matter (Lecture 2).

Numerical matching exercise

Choose $R = 2.0\,\mathrm{fm}$ and solve for the well depth V_0 that reproduces $B_d = 2.224\,\mathrm{MeV}$ with reduced mass $\mu = m_N/2$. Then repeat for $R = 1.5$ and $R = 2.5\,\mathrm{fm}$. The curve $V_0(R)$ falls as R grows: many wells share one binding energy. Overlay the mean-square radius for each solution and observe that radius and depth move together. That plot is the geometric content of Lecture 7's underdetermination statement.

Next, estimate the asymptotic decay constant $\gamma = \sqrt{2\mu B_d}/\hbar \approx 0.23\,\mathrm{fm}^{-1}$ and the exterior scale $1/\gamma \approx 4.3\,\mathrm{fm}$. Most of the probability density sits outside a 2 fm well, which is why low-energy scattering (Lecture 10) and peripheral transfer (Lecture 21) care about the asymptotic normalisation more than about the interior well shape. When Lecture 9 introduces the tensor force, interior physics returns for Q_d; until then, long-distance deuteron physics is deliberately simple.

Research frontier: EFT deuteron physics and student projects

The square-well deuteron of Lecture 7 teaches matching of interior and exterior wave functions and the consequences of weak binding. Modern few-body physics replaces that toy well by pionless and chiral EFTs that expand systematically in momenta over the breakdown scale, with quantified truncation errors [41, 42]. Lattice QCD is beginning to constrain low-energy constants that enter those EFTs, while precision deuteron observables (rms radius, quadrupole moment, photodisintegration, and electrodisintegration) benchmark the force. The pedagogical lesson survives: one binding energy cannot fix two potential parameters without additional data or a power-counting principle. Open research questions include the consistent inclusion of electromagnetic currents at the same chiral order as the Hamiltonian, the size of relativistic corrections, and how far pionless EFT can be pushed before explicit pions become mandatory. Connecting lattice-QCD phase shifts and deuteron properties to chiral LECs remains a multi-year programme rather than a finished calculation.

Students should also notice the difference between a potential that merely fits B_d and an EFT that predicts a tower of observables with truncation errors. Comparing a square-well deuteron to a published chiral calculation of the same radius and quadrupole moment is a concrete way to see what “systematic improvability” means in practice.

Student directions. (1) Computational: solve the square-well matching condition for several R and plot the $V_0(R)$ curve. (2) Analytic limit: estimate the exterior probability $P_>$ as $B_d \to 0$ and discuss halo formation. (3) Literature reading: from a chiral-EFT review, list which orders first generate a tensor force and a three-nucleon force [41].

1.11 Problems with solutions

Problem 7.1 — Binding energy of the deuteron

Atomic masses: $m(^1\mathrm{H}) = 1.007825\,\mathrm{u}$, $m(n) = 1.008665\,\mathrm{u}$, $m(^2\mathrm{H}) = 2.014102\,\mathrm{u}$. With $c^2 = 931.5\,\mathrm{MeV/u}$, compute B_d and B_d/A.

Solution 7.1

$$
\begin{aligned}
B_d &= [m(^1\mathrm{H}) + m(n) - m(^2\mathrm{H})]c^2 \\
&= (1.007825 + 1.008665 - 2.014102) \times 931.5\,\mathrm{MeV} \\
&= 0.002388 \times 931.5\,\mathrm{MeV} \approx 2.224\,\mathrm{MeV}.
\end{aligned}
$$

$$
B_d/A \approx 1.11\,\mathrm{MeV},
$$

much less than the mid-mass $\sim 8\,\mathrm{MeV}$ per nucleon: the deuteron is barely bound [6, 14].

Problem 7.2 — Solve the labelled square well

For $R = 2.00\,\text{fm}$, $B_d = 2.2246\,\text{MeV}$, and $\hbar^2/(2\mu) = 41.5\,\text{MeV fm}^2$, solve $\xi \cot \xi = -\eta$, where $\eta = R\sqrt{B_d/[\hbar^2/(2\mu)]}$, on the first-state branch $\pi/2 < \xi < \pi$. Determine V_0.

Solution 7.2

$$\eta = 2.00\sqrt{\frac{2.2246}{41.5}} = 0.463.$$

Numerical solution of $\xi \cot \xi = -0.463$ gives $\xi = 1.820$. Hence

$$V_0 = B_d + \frac{\hbar^2}{2\mu}\frac{\xi^2}{R^2} = 2.2246 + 41.5\frac{(1.820)^2}{(2.00)^2} \approx 36.6\,\text{MeV}.$$

This value belongs to the explicitly labelled $R = 2.00\,\text{fm}$ teaching model; B_d alone fixes a curve $V_0(R)$, not a unique potential [6].

Problem 7.3 — Bound-state condition V_0R^2 (Basdevant)

For an s-wave square well, at least one bound state requires $V_0R^2 > \pi^2\hbar^2/(8\mu) \approx 109\,\text{MeV fm}^2$. (a) With $R = 1.73\,\text{fm}$ and $V_0 = 46.7\,\text{MeV}$ (triplet fit), compute V_0R^2 and compare with $109\,\text{MeV fm}^2$. (b) The singlet channel has $V_0R^2 \sim 93.5\,\text{MeV fm}^2$. What does that imply?

Solution 7.3

(a)

$$V_0R^2 = 46.7 \times (1.73)^2 \approx 46.7 \times 2.99 \approx 140\,\text{MeV fm}^2 > 109\,\text{MeV fm}^2.$$

The triplet well is above threshold and binds the deuteron ($V_0R^2 \approx 140\,\text{MeV fm}^2$ reproduces $B_d = 2.225\,\text{MeV}$) [14].

(b) $93.5 < 109$: the singlet well is just *below* threshold. There is no bound ${}^1S_0$ pn state; low-energy singlet scattering shows a virtual state [14, 6].

Problem 7.4 — Normalisation and exterior probability

With $B_d = 2.224\,\text{MeV}$ and $\hbar^2/m_N = 41.5\,\text{MeV fm}^2$, compute $\gamma = \sqrt{2\mu B_d}/\hbar = \sqrt{m_N B_d}/\hbar$ and the decay length $1/\gamma$. For $R = 2.00\,\text{fm}$ and $kR = 1.820$, use

$$A^{-2} = \frac{R}{2} - \frac{\sin(2kR)}{4k} + \frac{\sin^2(kR)}{2\gamma}, \qquad P_> = \frac{A^2\sin^2(kR)}{2\gamma}$$

to find the probability outside the well.

Solution 7.4

$$\gamma = \sqrt{\frac{m_N B_d}{\hbar^2}} = \sqrt{\frac{B_d}{\hbar^2/m_N}} = \sqrt{\frac{2.224}{41.5}} \approx \sqrt{0.0536} \approx 0.231\,\text{fm}^{-1}.$$

$$\frac{1}{\gamma} \approx 4.3\,\text{fm} > R = 2.00\,\text{fm}.$$

With $k = 1.820/R = 0.910\,\text{fm}^{-1}$,

$$A^{-2} \approx 3.16\,\text{fm}, \qquad P_{>} \approx 0.642.$$

About 64% of the radial probability lies outside the force range: the deuteron is a loosely bound, extended system [6, 14].

Problem 7.5 — Thermal deuterons (Petrera 1.1.4)

Estimate the temperature at which two deuterons can approach to $r \sim 1\,\text{fm}$ against Coulomb repulsion. Use $k_B = 8.6 \times 10^{-5}\,\text{eV/K}$ and $\alpha\,\hbar c \approx 1.44\,\text{MeV fm}$.

Solution 7.5

In the rest frame of one deuteron the other approaches with relative velocity $2v$, so

$$4k_B T \sim \frac{\alpha\,\hbar c}{r} \approx \frac{1.44}{1} = 1.44\,\text{MeV}.$$

$$T \sim \frac{1.44 \times 10^{6}\,\text{eV}}{4 \times 8.6 \times 10^{-5}\,\text{eV/K}} \sim 4 \times 10^{9}\,\text{K}.$$

Nuclear contact among charged light nuclei requires stellar temperatures [3].

Problem 7.6 — Photodisintegration threshold

The $\gamma + {}^2\text{H} \to p + n$ threshold is essentially B_d plus a small centre-of-mass correction. If a photon of energy $E_\gamma = 2.50\,\text{MeV}$ breaks a deuteron at rest, what is the total kinetic energy of the $p + n$ system in the lab (neglect recoil of the compound system before breakup, to leading order)?

Solution 7.6

Energy conservation:

$$E_\gamma = B_d + T_p + T_n \quad \Rightarrow \quad T_p + T_n = 2.50 - 2.224 = 0.276\,\text{MeV}.$$

The excess photon energy above threshold appears as kinetic energy of the two nucleons [6].

Bibliography

[1] R. A. Dunlap, *An Introduction to the Physics of Nuclei and Particles* (2nd ed.), IOP Publishing, Bristol (2023), DOI: 10.1088/978-0-7503-6094-4, Ch. 3 (Nuclear composition and size).

[2] W. Demtröder, *Nuclear and Particle Physics*, Undergraduate Lecture Notes in Physics, Springer, Cham (2023).

[3] S. Petrera, *Problems and Solutions in Nuclear and Particle Physics*, UNITEXT for Physics, Springer, Cham (2019).

[4] F. Terranova, *A Modern Primer in Particle and Nuclear Physics*, Oxford University Press (2021).

[5] S. D'Auria, *Introduction to Nuclear and Particle Physics*, Undergraduate Lecture Notes in Physics, Springer, Cham (2018).

[6] K. S. Krane, *Introductory Nuclear Physics*, Wiley, New York (1988).

[7] R. Hofstadter, "Electron scattering and nuclear structure," Rev. Mod. Phys. **28**, 214 (1956).

[8] H. F. Ehrenberg, R. Hofstadter, U. Meyer-Berkhout, D. G. Ravenhall, and S. E. Sobottka, "High-Energy Electron Scattering and the Charge Distribution of Carbon-12 and Oxygen-16," Phys. Rev. **113**, 666 (1959).

[9] H. Yukawa, "On the interaction of elementary particles. I," Proc. Phys.-Math. Soc. Japan **17**, 48 (1935).

[10] R. D. Woods and D. S. Saxon, "Diffuse surface optical model for nucleon-nuclei scattering," Phys. Rev. **95**, 577 (1954).

[11] H. G. J. Moseley, "The high-frequency spectra of the elements," Phil. Mag. **26**, 1024 (1913); **27**, 703 (1914).

[12] C. F. von Weizsäcker, "Zur Theorie der Kernmassen," Z. Phys. **96**, 431 (1935).

[13] P. Cappellaro, *Introduction to Applied Nuclear Physics* (MIT OpenCourseWare / LibreTexts), CC BY-NC-SA 4.0.

[14] J.-L. Basdevant, J. Rich, and M. Spiro, *Fundamentals in Nuclear Physics: From Nuclear Structure to Cosmology*, Springer, New York (2005).

[15] D. Tong, *Particle Physics*, Lecture notes (University of Cambridge / CERN school notes).

[16] M. G. Mayer, "On closed shells in nuclei. II," Phys. Rev. **75**, 1969 (1949).

[17] O. Haxel, J. H. D. Jensen, and H. E. Suess, "On the "magic numbers" in nuclear structure," Phys. Rev. **75**, 1766 (1949).

[18] T. Schmidt, "Über die magnetischen Momente der Atomkerne," Z. Phys. **106**, 358 (1937).

[19] L. W. Nordheim, "On spins, moments, and shells in nuclei," Phys. Rev. **78**, 294 (1950).

[20] Evaluated Nuclear Structure Data File (ENSDF), National Nuclear Data Center, Brookhaven National Laboratory, `https://www.nndc.bnl.gov/ensdf/`.

[21] NuDat 3, National Nuclear Data Center, Brookhaven National Laboratory, `https://www.nndc.bnl.gov/nudat3/`.

[22] N. J. Stone, "Table of nuclear magnetic dipole and electric quadrupole moments," At. Data Nucl. Data Tables **90**, 75 (2005); updated compilations at NNDC.

[23] W. N. Cottingham and D. A. Greenwood, *An Introduction to Nuclear Physics* (2nd ed.), Cambridge University Press, Cambridge (2001).

[24] H. Geiger and J. M. Nuttall, "The ranges of the α particles from the radioactive substances," Phil. Mag. **22**, 613 (1911).

[25] G. Gamow, "Zur Quantentheorie des Atomkernes," Z. Phys. **51**, 204 (1928).

[26] R. W. Gurney and E. U. Condon, "Wave mechanics and radioactive disintegration," Nature **122**, 439 (1928); Phys. Rev. **33**, 127 (1929).

[27] M. Wang, W. J. Huang, F. G. Kondev, G. Audi, and S. Naimi, "The AME 2020 atomic mass evaluation (II). Tables, graphs and references," Chin. Phys. C **45**, 030003 (2021).

[28] Laboratoire National Henri Becquerel (LNHB), Recommended decay data, `http://www.lnhb.fr/nuclear-data/nuclear-data-table/`.

[29] L. M. Langer, R. D. Moffat, and H. C. Price, Jr., "Low energy beta-ray spectra: P^{32} and Cu^{64}," Phys. Rev. **76**, 1725 (1949).

[30] L. M. Langer and H. C. Price, Jr., "Shapes of the beta-spectra of the forbidden transitions of Sb^{124}, Rb^{86}, Sr^{89}, Y^{91}, and Cs^{137}," Phys. Rev. **75**, 1769 (1949).

[31] D. C. Camp and L. M. Langer, "The shape of the ^{66}Ga positron spectrum and the contribution from $0^+ \to 0^+$ transitions," Phys. Rev. **129**, 1782 (1963).

[32] H. C. Verma, *Nuclear Physics: Fundamentals and Applications*, NPTEL/IIT Kanpur lecture series, `https://hcverma.in/ncl_phy_lectures`.

[33] International Atomic Energy Agency, *LiveChart of Nuclides*, evaluated structure, decay, reaction, and fission-yield data, `https://www-nds.iaea.org/relnsd/vcharthtml/VChartHTML.html`.

[34] T. Kibédi, T. W. Burrows, M. B. Trzhaskovskaya, P. M. Davidson, and C. W. Nestor, Jr., "Evaluation of theoretical conversion coefficients using BrIcc," Nucl. Instrum. Methods Phys. Res. A **589**, 202 (2008), DOI: 10.1016/j.nima.2008.02.051.

[35] D. A. Brown *et al.*, "ENDF/B-VIII.0: The 8th major release of the nuclear reaction data library with CIELO-project cross sections, new standards and thermal scattering data," Nucl. Data Sheets **148**, 1 (2018), DOI: 10.1016/j.nds.2018.02.001.

[36] B. Acharya *et al.*, "Solar fusion III: New data and theory for hydrogen-burning stars," Rev. Mod. Phys. **97**, 035002 (2025), DOI: 10.1103/8lm7-gs18.

[37] S. N. Ghoshal, "An experimental verification of the theory of compound nucleus," Phys. Rev. **80**, 939 (1950), DOI: 10.1103/PhysRev.80.939.

[38] D. Adhikari *et al.* (PREX Collaboration), "Accurate determination of the neutron skin thickness of ^{208}Pb through parity-violation in electron scattering," Phys. Rev. Lett. **126**, 172502 (2021), DOI: 10.1103/PhysRevLett.126.172502.

[39] B. T. Reed, F. J. Fattoyev, C. J. Horowitz, and J. Piekarewicz, "Implications of PREX-II on the equation of state of neutron-rich matter," Phys. Rev. Lett. **126**, 172503 (2021), DOI: 10.1103/PhysRevLett.126.172503.

[40] B. Hu *et al.*, "Ab initio predictions link the neutron skin of ^{208}Pb to nuclear forces," Nature Phys. **18**, 1196 (2022), DOI: 10.1038/s41567-022-01715-8.

[41] E. Epelbaum, H.-W. Hammer, and U.-G. Meißner, "Modern theory of nuclear forces," Rev. Mod. Phys. **81**, 1773 (2009), DOI: 10.1103/RevModPhys.81.1773.

[42] H.-W. Hammer, S. König, and U. van Kolck, "Nuclear effective field theory: Status and perspectives," Rev. Mod. Phys. **92**, 025004 (2020), DOI: 10.1103/RevModPhys.92.025004.

[43] T. Otsuka, A. Gade, O. Sorlin, T. Suzuki, and Y. Utsuno, "Evolution of shell structure in exotic nuclei," Rev. Mod. Phys. **92**, 015002 (2020), DOI: 10.1103/RevModPhys.92.015002.

[44] H. Hergert, S. K. Bogner, T. D. Morris, A. Schwenk, and K. Tsukiyama, "The in-medium similarity renormalization group: A novel ab initio method for nuclei," Phys. Rep. **621**, 165 (2016), DOI: 10.1016/j.physrep.2015.12.007.

[45] J. M. Lattimer and M. Prakash, "The equation of state of hot, dense matter and neutron stars," Phys. Rep. **621**, 127 (2016), DOI: 10.1016/j.physrep.2015.12.005.

[46] J. M. Lattimer, "Neutron stars and the nuclear matter equation of state," Annu. Rev. Nucl. Part. Sci. **71**, 433 (2021), DOI: 10.1146/annurev-nucl-102419-124827.

[47] B. P. Abbott *et al.* (LIGO Scientific Collaboration and Virgo Collaboration), "GW170817: Observation of gravitational waves from a binary neutron star inspiral," Phys. Rev. Lett. **119**, 161101 (2017), DOI: 10.1103/PhysRevLett.119.161101.

[48] M. J. Dolinski, A. W. P. Poon, and W. Rodejohann, “Neutrinoless double-beta decay: Status and prospects,” Annu. Rev. Nucl. Part. Sci. **69**, 219 (2019), DOI: 10.1146/annurev-nucl-101918-023407.

[49] M. Agostini, G. Benato, J. A. Detwiler, J. Menéndez, and F. Vissani, “Toward the discovery of matter creation with neutrinoless $\beta\beta$ decay,” Rev. Mod. Phys. **95**, 025002 (2023), DOI: 10.1103/RevModPhys.95.025002.

[50] P. Gysbers *et al.*, “Discrepancy between experimental and theoretical β-decay rates resolved from first principles,” Nature Phys. **15**, 428 (2019), DOI: 10.1038/s41567-019-0450-7.

[51] H. L. Crawford, K. Fossez, S. König, and A. Spyrou, “A vision for the science of rare isotopes,” Annu. Rev. Nucl. Part. Sci. **74**, 141 (2024), DOI: 10.1146/annurev-nucl-121423-091501.

[52] Nuclear Science Advisory Committee, *A New Era of Discovery: The 2023 Long Range Plan for Nuclear Science*, U.S. Department of Energy and National Science Foundation (2023), `https://nuclearsciencefuture.org/`.

[53] S. A. Giuliani, Z. Matheson, W. Nazarewicz, E. Olsen, P.-G. Reinhard, J. Sadhukhan, B. Schuetrumpf, N. Schunck, and P. Schwerdtfeger, “Colloquium: Superheavy elements: Oganesson and beyond,” Rev. Mod. Phys. **91**, 011001 (2019), DOI: 10.1103/RevModPhys.91.011001.

[54] N. Schunck and D. Regnier, “Theory of nuclear fission,” Prog. Part. Nucl. Phys. **125**, 103963 (2022), DOI: 10.1016/j.ppnp.2022.103963.

[55] I. Counts, J. Hur, D. P. L. Aude Craik, H. Jeon, C. Leung, J. C. Berengut, A. Geddes, A. Kawasaki, W. Jhe, and V. Vuletić, “Evidence for nonlinear isotope shift in Yb^{+} search for new boson,” Phys. Rev. Lett. **125**, 123002 (2020), DOI: 10.1103/PhysRevLett.125.123002.

[56] I. Angeli and K. P. Marinova, “Table of experimental nuclear ground state charge radii: An update,” At. Data Nucl. Data Tables **99**, 69 (2013), DOI: 10.1016/j.adt.2011.12.006.

[57] S. Kraemer *et al.*, “Observation of the radiative decay of the ^{229}Th nuclear clock isomer,” Nature **617**, 706 (2023), DOI: 10.1038/s41586-023-05894-z.